PSFC/JA-99-3

Modeling of Particle and Energy Transprot in the Edge Plasma of Alcator C-Mod

M.V. Umansky, S.I. Krasheninnikov,
B. LaBombard, B. Lipschultz, J.L. Terry

January 1999

Plasma Science and Fusion Center
Massachusetts Institute of Technology
Cambridge, MA 02139

To be published in Physics of Plasmas.

This work was supported in part by the U. S. Department of Energy Contract No. DE-AC02-78ET51013. Reproduction, translation, publication, use and disposal, in whole or in part by or for the United States government is permitted.

January 12, 1999

Modeling of particle and energy transport in the edge plasma of Alcator C-Mod.

M.V.Umansky, S.I.Krasheninnikov, B.LaBombard,
B.Lipschultz and J.L.Terry

Plasma Science and Fusion Center
Massachusetts Institute of Technology
Cambridge, Massachusetts 02139

In the present study recycling and transport in the edge plasma of Alcator C-Mod [I.H.Hutchinson et al., Phys.Plasmas 1, 1511 (1994)] is modeled and analyzed with the multi-fluid code UEDGE [T.D.Rognlien et al., J. Nucl. Mat., 196, (1992)]. Matching the experimental plasma density profiles in the scrape-off layer (SOL) requires a spatially dependent effective anomalous diffusion coefficient $D_\perp$ growing rapidly towards the wall. The mid-plane pressure of neutral gas, P_{mid}, is a key parameter that reflects the magnitude of anomalous transport of plasma from the core. Recycling of plasma on the main chamber wall appears to be quite significant, especially in the case of high $P_{mid} \sim 0.3$ mTorr when the main wall provides $\sim 70\%$ of recycling neutrals in the main chamber. In the upper SOL (well above the x-point) draining of particles by the poloidal flow is weak and thus the particle balance is predominantly radial. For the radial heat transport it is found that energy flux carried by radial plasma convection and by charge-exchange (CX) neutrals is quite significant in SOL. In the high P_{mid} case, heat conduction by CX neutrals along with radial heat convection by plasma carries most of the power flux (~ 75 %) across the last closed flux surface. In the low P_{mid} case, heat conduction by CX neutrals dominates the radial heat flux far out in the SOL.

PACS 52.55.Fa, 52.40.Hf, 52.65.Kj

I. Introduction

The physics of plasma recycling and core fueling in the tokamak is of primary importance for the present and next generation fusion devices. However, the present level of understanding of these processes is still insufficient. In the traditionally accepted picture[1–3] of particle transport in the edge plasma in a divertor tokamak, all ions flowing out of the core are assumed to be brought to the divertor by the parallel flow in the scrape-off layer (SOL). However it has been recently recognized[4] that the processes of plasma recycling and core fueling in the Alcator C-Mod tokamak[5] look very different than in the traditional picture. As shown in our earlier paper[4] the spectroscopic data indicates that in the main chamber of Alcator C-Mod there exists a significant plasma source (up to $10^{23}s^{-1}$) due to ionization of neutrals. Mach probe data indicates that the parallel plasma flow in the SOL of Alcator C-Mod is by far too weak to channel such a large flow of ions into the divertor. Thus in Alcator C-Mod plasmas a large fraction of ions flowing out of the core recycle in the main chamber rather than in the divertor. To investigate further particle and energy transport in the edge plasma of Alcator C-Mod, the present work provides numerical modeling of C-Mod with the multi-fluid code UEDGE.[6]

II. Modeling of radial profiles of plasma density and temperature in scrape-off layer

The present study is focused primarily on the transport behavior of the scrape-off layer (SOL). Consequently, the modeling is done in a simplified curvilinear orthogonal geometry convenient for studying the SOL. A locally orthogonal computational mesh covers a domain representing the edge plasma of C-Mod (see Fig. 1). Using UEDGE, we numerically solve the steady-state Braginskii fluid equations[7] for ions and electrons and the Navier-Stokes equation for the neutrals. The drift terms and the electric field are neglected for computational simplicity.

The external boundary of the computational domain is modeled as a fully recycling material wall. This implies coupling of radial flux density for ions and neutrals at the wall, and also coupling of the radial heat flux at the wall with local plasma and neutral densities and temperatures through the heat transmission coefficients. This sets the boundary conditions for the plasma,

neutral density, and energy equations at the wall.

At the inner boundary of the computational domain (the core interface) the input power and plasma density are specified providing the boundary conditions for the plasma energy and density equations. The boundary condition for the neutral density equation at the core interface is provided by setting neutral particle flux density to zero. Note that this set of boundary conditions automatically provides zero plasma flux through the core interface in a steady state. The latter is physically justified for Alcator C-Mod where a steady state is achieved without fueling of the core by pellets or a neutral beam.

In the present modeling it is found that it is impossible to match the experimental radial profile of plasma density in the SOL using a spatially uniform anomalous plasma diffusion coefficient $D_\perp$. As an illustrative case, we solve for 2-D plasma profiles using UEDGE with various values of spatially constant anomalous plasma diffusion coefficient $D_\perp$. In all cases, the cross-field plasma density profile in SOL appears to have the wrong curvature for various values of $D_\perp$ as shown in Fig. 2. The main reason for this is a large ionization source in SOL due to high neutral density there. Matching the plasma density profiles in the SOL turns out to be possible by using a plasma diffusion coefficient which grows radially towards the wall.

In the present work two C-Mod discharges were modeled: shot 950607021 with core plasma density $\bar{n}_e \approx 2.4 \times 10^{20} m^{-3}$ and relatively high mid-plane gas pressure, $P_{mid} \approx 0.3$ mTorr, and shot 960208031 with core plasma density $\bar{n}_e \approx 1.2 \times 10^{20} m^{-3}$ and low $P_{mid} \approx 0.025$ mTorr. Both shots are Ohmic L-modes with parameters typical for C-Mod operations: plasma current $I_p \approx$ 0.8 MA and the power flow across the separatrix into the SOL $P_{sol} \approx 0.7$ MW. For both shots the SOL profiles of plasma density and temperature look quite typical for C-Mod.

In the modeling the input power P_{sol} was set close (within 25 %) to the experimentally inferred value. The anomalous plasma diffusion coefficient $D_\perp(\rho)$ as a function of the flux surface and the anomalous plasma heat diffusivity $\chi_\perp$ ($\chi_{\perp i} = \chi_{\perp e} = \chi_\perp$) for plasma were adjusted to match profiles of the electron density and temperature in SOL to that measured by a fast-scanning probe (FSP).[10]

A spatially constant plasma heat diffusivity $\chi_\perp$ sufficed to achieve a reasonably good match with the experimental electron temperature profiles. The value of $\chi_\perp$ is 0.1 m^2/s for the high P_{mid} case and 0.5 m^2/s for the low P_{mid}

case.

For both shots the mid-plane gas pressure was matched within 25 %. The mid-plane pressure P_{mid} in these calculations was inferred from the neutral temperature and density at the wall assuming the kinetic flux balance between the molecules in the pressure gauge and the atoms near the wall. For both modeled discharges the chord-integrated D_α brightness for a horizontal view through the mid-plane of the plasma turned out to be smaller than the experimental value by a factor of about 3. We have not, as yet, been able to determine the primary cause of this discrepancy. It may be due to utilization of a simple fluid model for the neutrals instead of a kinetic treatment which would be more appropriate here since the mean free path for the neutrals is comparable to the width of the SOL. Also it is possible that reflections of light from the walls of the vessel amplify to some extent the D_α brightness. Another possible reason is that the way of interpreting the pressure gauge data using kinetic balance arguments may be not quite accurate due to the complicated geometry of the gauge.

The results of matching of experimental plasma density and temperature profiles are shown in Fig. 3 and Fig. 4. A good match with the experimental SOL density profiles could be achieved also by using a spatially uniform $D_\perp$ combined with a spatially uniform radial inward pinch, or by using a radially growing outward radial "anti-pinch".

III. Particle flux balance and core fueling

Part of SOL	$\Gamma_{wall}[s^{-1}]$		$\Gamma_{sepx}[s^{-1}]$		$\Gamma_{bot}[s^{-1}]$	
	ion	neutral	ion	neutral	ion	neutral
Main	$7.9\ 10^{20}$	$-7.9\ 10^{20}$	$6.9\ 10^{20}$	$-3.3\ 10^{20}$	$4.2\ 10^{20}$	$-6.7\ 10^{19}$
X-pt	$6.9\ 10^{19}$	$-6.9\ 10^{19}$	$1.9\ 10^{20}$	$-5.4\ 10^{20}$	$2.6\ 10^{21}$	$-2.6\ 10^{21}$
Whole	$8.6\ 10^{20}$	$-8.6\ 10^{20}$	$8.7\ 10^{20}$	$-8.7\ 10^{20}$	$2.6\ 10^{21}$	$-2.6\ 10^{21}$

Table 1: Particle flux balance in the low P_{mid} case

To analyze transport of particles in the edge plasma it is convenient to consider separately the "main SOL" domain and the "X-point SOL" domain which are defined as shown in Fig. 5. The main SOL is the part of the SOL above the level of the scanning probe which makes this definition convenient for benchmarking of the modeling against the probe data. The X-point SOL

Part of SOL	$\Gamma_{wall}[s^{-1}]$		$\Gamma_{sepx}[s^{-1}]$		$\Gamma_{bot}[s^{-1}]$	
	ion	neutral	ion	neutral	ion	neutral
Main	$2.7\ 10^{22}$	$-2.7\ 10^{22}$	$1.1\ 10^{22}$	$-5.4\ 10^{21}$	$6.3\ 10^{21}$	$-1.0\ 10^{21}$
X-pt	$1.6\ 10^{22}$	$-1.6\ 10^{22}$	$2.9\ 10^{21}$	$-8.2\ 10^{21}$	$1.9\ 10^{22}$	$-1.9\ 10^{22}$
Whole	$4.2\ 10^{22}$	$-4.2\ 10^{22}$	$1.4\ 10^{22}$	$-1.4\ 10^{22}$	$1.9\ 10^{22}$	$-1.9\ 10^{22}$

Table 2: Particle flux balance in the high P_{mid} case

is the lower part of the SOL. The "whole SOL" domain is the union of the main SOL and the X-point SOL. The lower poloidal edge of each domain is defined as its "bottom". For the main SOL the bottom is the boundary between the main SOL and the X-point SOL. For both the X-point SOL and the whole SOL, the bottom is the boundary between the main chamber and the divertor chamber. For each of the three domains (main SOL, X-point SOL and the whole SOL) we consider poloidal particle fluxes through the bottom, Γ_{bot}, and radial particle fluxes through the outer wall boundary, Γ_{wall}, and through the separatrix, Γ_{sepx}. Approximate values of these fluxes for ions and neutrals are presented in Table 1 and Table 2 for the low P_{mid} and the high P_{mid} cases respectively. Positive sign is assumed for Γ_{wall} directed towards the outer wall, for Γ_{sepx} directed out of the core and for Γ_{bot} directed towards the divertor.

First, analyzing particle balance for the whole SOL domain using Tables 1 and 2, one can see that in both cases the total flux of ions escaping to the wall and into the divertor, $\Gamma_{wall} + \Gamma_{bot}$, is by far larger than the ion flux entering the SOL from the core, Γ_{sepx}. This means that neutral fueling of the SOL is much larger than neutral fueling of the core. For the ionization source above the X-point level the fraction of it which is located inside the last closed flux surface (LCFS) is given by the ratio $\Gamma_{sepx}/(\Gamma_{wall} + \Gamma_{bot})$ which is about 0.2 for both the high P_{mid} and the low P_{mid} cases.

Next, compare the magnitudes of Γ_{wall} and Γ_{bot} for the whole SOL. In the low P_{mid} case Γ_{bot} is by a factor of ~ 3 larger than Γ_{wall} which means that the ionization source in the main chamber is primarily balanced by the poloidal ion flux into the divertor. However, in the high P_{mid} case Γ_{wall} is by a factor of ~ 2 greater than Γ_{bot} and thus recycling of plasma on the main wall becomes an important player in the particle balance. Note that in some C-Mod discharges the magnitude of P_{mid} can reach values as high as a few mTorr. It seems likely that for such cases of extremely high P_{mid} recycling

of plasma on the main wall completely dominates the particle balance in the SOL.

Examining the particle fluxes in Tables 1 and 2 for the main SOL one can see that in both high P_{mid} and low P_{mid} cases the ion and neutral particle fluxes through the bottom of the main SOL cannot balance particle fluxes flowing in the radial direction. A large ion flux to the outer wall is sustained by a significant ionization source in the main SOL. Thus in the main SOL the particle balance is predominantly radial even in the low P_{mid} case.

The poloidal ion flux through the divertor throat, Γ_{bot} for the whole SOL, is much larger than Γ_{bot} for the main SOL. This is because of a large ionization source in the X-point SOL domain. As it can be seen from Table 2 in the high P_{mid} case, the lower part of the main wall takes a large fraction of the wall particle flux.

It is important that the parallel flow appears to be a secondary effect for the particle balance in the main SOL. The calculated poloidal ion flux through the bottom of the main SOL can be compared with the experiment since both plasma density and parallel velocity data are available from the Mach probe. Typically, the parallel velocity of plasma flow in SOL is 1-10 km/s in C-Mod according to the probe.[10] In the present modeling it is found that the parallel velocity near the probe's location in SOL has the right order of magnitude. Since we are matching quite accurately the density profiles in the SOL the calculated poloidal ion flux at the bottom of the main SOL should also have the right order of magnitude.

The poloidal distribution of particle flux density across LCFS is shown in Fig. 6. The radial particle flux density at the separatrix scaled by a factor $2\pi R$ (evaluated locally) is plotted as a function of the poloidal distance along separatrix. The x-coordinate starts from the X-point and follows clockwise along the separatrix coming back to the X-point. One can see in Fig. 6 that the contribution to the radial ion flux is larger at the outer side. This is mainly because at the outer side the compression of magnetic surfaces is larger. Fig. 6 and Tables 1 and 2 demonstrate that the core plasma is fueled to a large extent by neutrals penetrating through the lower part of the LCFS.

In the modeling for the low P_{mid} case we find that poloidal plasma flow at the separatrix is directed out of the divertor in both the inner and the outer SOL regions. A reverse flow at the separatrix is often seen in C-Mod experiments in the outer SOL[10] but no data is available for the inner side. One should note that in C-Mod the parallel flow in the SOL and the reverse flow in

particular depends on the direction of the toroidal magnetic field which is apparently related to the plasma drifts.[8] This feature cannot be examined in the present modeling since drifts are not included here.

IV. Radial heat transport

The radial heat flux in the model is given by

$$q_{tot} = q_{anom} + q_{ecnv} + q_{incnv} + q_{cx} \tag{1}$$

where q_{anom} is the flux due to the anomalous radial heat conduction by plasma, q_{ecnv} is the radial heat flux convected by electrons, q_{incnv} is the radial heat flux convected by ions and neutrals and q_{cx} is the heat flux conducted by the neutrals.
The anomalous heat flux conducted by the plasma is

$$q_{anom} = -n_e \chi_\perp \nabla_\perp T_e - n_i \chi_\perp \nabla_\perp T_i \tag{2}$$

where n_e and n_i are densities of electrons and ions, T_e and T_i are the temperatures, $\chi_\perp$ is the anomalous heat diffusivity.
The heat flux conducted by neutrals is given by

$$q_{cx} = -\kappa_{cx} \nabla_\perp T_i \tag{3}$$

where κ_{cx} is the heat conductivity associated with the presence of neutrals in plasma (mainly due to the charge-exchange processes)

$$\kappa_{cx} \approx n_n \lambda_{cx}^2 \nu_{cx} \approx \frac{n_n}{n_i \sigma_{cx}} V_{tn} \tag{4}$$

where V_{tn} is the neutral thermal velocity, n_n the neutral density, λ_{cx} is the mean free path of charge-exchange, ν_{cx} is the frequency of charge-exchange. In an attempt to make a correction for kinetic effects it is possible to use a flux-limiting factor for κ_{cx}

$$\kappa_{cx}^{fl} = \frac{\kappa_{cx}}{1 + |C \frac{\lambda_{cx}}{\lambda_T}|} \tag{5}$$

where λ_T is a characteristic scale of radial temperature variation and C is a constant of the order of unity. In comparing calculations done with and

without such a flux-limiting factor, we found that all results are quite similar. All plots and numbers presented in this report are taken from code runs where no flux-limiting factor was used.
The radial heat flux convected by electrons is

$$q_{ecnv} = \frac{5}{2} T_e j_{rp} \tag{6}$$

and the radial heat flux convected by ions and neutrals is

$$q_{incnv} = \frac{5}{2} (T_i j_{rp} + T_n j_{rn}) \tag{7}$$

where T_n is the neutral temperature, j_{rp} is the radial plasma flux density, j_{rn} is the radial neutral flux density. In some cases q_{incnv} may become negative due to slight imbalance between ion and neutral radial particle fluxes at a particular flux surface.
In Fig. 7 the total radial power flux across SOL and all its components (integrated over the flux surface above the x-point level) are plotted against the radial coordinate ρ, the distance from separatrix at mid-plane. One can see that in the high P_{mid} case convection of heat by plasma and heat conduction by CX neutrals dominate heat transport across the whole SOL. In the high P_{mid} case these two power channels account for $\sim 75\%$ of P_{sol}, the total power coming from the core.
In the low P_{mid} case convection of heat is small while heat conduction by CX neutrals dominates the radial heat flux starting from $\rho \approx 3$ mm.
In the low P_{mid} case the neutral density near the wall is by a factor of ~ 10 smaller than in the high P_{mid} case. However the effect of heat conduction by CX neutrals is still quite significant in the low P_{mid} case since the plasma density in SOL is roughly proportional to P_{mid} which makes κ_{cx} vary only slightly.

V. Discussion

Two features of the anomalous particle transport represented by an effective diffusion coefficient $D_\perp$ are evident from the present modeling. First, the profiles of $D_\perp$ are very similar in both the low P_{mid} and the high P_{mid} cases with the effective $D_\perp$ growing rapidly across SOL. This suggests that a mechanism different from diffusion governs the anomalous particle transport

in SOL.[4] Second, the magnitude of $D_\perp$ is much larger in the high P_{mid} case. The data presented in Fig. 8 shows that the mid-plane pressure P_{mid} grows roughly as the cubic power of the core plasma density $\bar{n}_e$ in L-modes. Thus the plasma transport from the core also grows quite rapidly with the core density. This implies existence of a core density limit above which plasma in L-mode cannot be sustained in this machine because of overwhelming heat losses.

The data presented in Fig. 8 shows that the mid-plane gas pressure P_{mid} scales with the core density quite differently in L-modes than in H-modes. This suggests that P_{mid} is related to intrinsic properties of the plasma and in particular the anomalous particle transport.

It is not clear yet whether the picture of particle transport and core fueling in other tokamaks is similar to what we find here for C-Mod. Note that C-Mod occupies a unique position among other tokamaks due to its molybdenum walls, high core density, high magnetic field and compact size. It is possible that the anomalous transport across the LCFS in C-Mod is higher than in other machines.

The result that higher mid-plane gas pressure is linked with higher levels of anomalous transport from the core is consistent with the observation made on C-Mod that P_{mid} is lower in H-modes.[9] For high P_{mid} heat convection and conduction by CX neutrals significantly enhance transport of heat from the core as shown by Fig. 7.

It has been observed that the neutral gas bypass in the Alcator C-Mod divertor has a strong effect on T_e profiles measured across SOL by the fast-scanning probe: with closing of the bypass the T_e profiles became steeper.[10] This can be a manifestation of the charge-exchange heat conduction in SOL. The bypass is geometrically close to the FSP and closure of the bypass might have lowered the local density of neutrals making the resulting cross-field heat diffusivity smaller.

VI. Conclusions

The present numerical modeling illustrates important features of the edge plasma in Alcator C-Mod. In the regime characterized by low P_{mid} ($\sim$ 0.01 mTorr) neutrals originating in the divertor chamber dominate the neutral population in the main chamber. However, in the regime characterized by high P_{mid} ($\sim$ 0.1-1 mTorr) recycling of plasma on the main chamber wall

provides most of neutrals present in the main chamber. Draining of plasma by the poloidal flow is not significant for the main SOL where the particle balance is mostly radial.

The mid-plane gas pressure P_{mid} reflects the magnitude of particle transport from the core. In L-modes the mid-plane gas pressure P_{mid} grows rapidly (approximately cubically) with the core density which indicates that the magnitude of plasma transport from the core grows rapidly with the core density.

In the high P_{mid} regime heat convection due to the radial plasma flow and heat conduction by CX neutrals dominate the cross-field heat transport across the SOL and carry most of power across LCFS. Even in the low P_{mid} regime heat conduction by CX neutrals dominates the cross-field heat transport far out ($\rho \gtrsim 3mm$) in SOL.

Acknowledgements

The authors would like to thank T.D.Rognlien for providing them with a great numerical tool (UEDGE) and many valuable discussions. This work is supported by U.S. Department of Energy Contract No. DE-AC02-78ET5103 and grant DE-FG02-92ER-54109.

References

[1]J.Wesson, "Tokamaks", Clarendon Press, Oxford, 1987

[2]P.C.Stangeby, in "Physics of Plasma-Wall Interactions in Controlled Fusion", p.41-98, Proceedings of a NATO Advanced Study Institute, Plenum Press, New York and London (1986).

[3]F.Wagner and K.Lackner, in "Physics of Plasma-Wall Interactions in Controlled Fusion", p.931-1004, Proceedings of a NATO Advanced Study Institute, Plenum Press, New York and London (1986).

[4]M.V.Umansky, S.I.Krasheninnikov, B.LaBombard, J.L.Terry, *Phys.Plasmas* **5**, 3373 (1998).

[5]I.H.Hutchinson, R.Boivin, F.Bombarda, P.Bonoli, S.Fairfax, C.Fiore, J.Goetz, S.Golovato, R.Granetz, M.Greenwald, S.Horne, A.Hubbard, J.Irby, B.LaBombard, B.Lipschultz, E.Marmar, G.McCracken, M.Porkolab, J.Rice, J.Snipes, Y.Takase, J.Terry, S.Wolfe, C.Christensen, D.Garnier, M.Graf, T.Hsu, T.Luke, M.May, A.Niemczewski, G.Tinios, J.Schachter, J.Urbahn, *Phys.Plasmas* **1**, 1511 (1994)

[6]T.D.Rognlien, J.L.Milovich, M.E.Rensink and G.D.Porter, *J. Nucl. Mat.* **196-198**, 347-351 (1992).

[7]S.I.Braginskii, Transport Processes in a Plasma, in *Reviews of Plasma Physics, v.1*, Consultants Bureau, New York, 1965.

[8]I.H.Hutchinson, B.LaBombard, J.A.Goetz, B.Lipschultz, G.M.McCracken, J.A.Snipes ang J.L.Terry, *Plasma Phys. Control Fusion* **36** 1389 (1995).

[9]Greenwald, M; Boivin, R L; Bonoli, P; Christensen, C; Fiore, C; Garnier, D; Goetz, J; Golovato, S; Graf, M; Granetz, R; Horne, S; Hsu, T; Hubbard, A; Hutchinson, I; Irby, J; Kurz, C; LaBombard, B; Lipschultz, B; Luke, T; Marmar, E; McCracken, G; Niemczewski, A; O'Shea, P; Porkolab, M; Rice, J; Reardon, J; Schachter, J; Snipes, J; Stek, P; Takase, Y; Terry, J; Umansky, M; Watterson, R; Wolfe, S; Bombarda, F; May, M; Welch, B *Phys.Plasmas* **2**, 2308 (1995).

[10]B. LaBombard, J.A. Goetz, I. Hutchinson, D. Jablonski, J. Kesner, C. Kurz, B. Lipschultz, G. M. McCracken, A. Niemczewski, J. Terry, A. Allen,

R.L. Boivin, F. Bombarda, P. Bonoli, C. Christensen, C. Fiore, D. Garnier, S. Golovato, R. Granetz, M. Greenwald, S. Horne, A. Hubbard, J. Irby, D. Lo, D. Lumma, E. Marmar, M. May, A. Mazurenko, R. Nachtrieb, H. Ohkawa, P. O'Shea, M. Porkolab, J. Reardon, J. Rice, J. Rost, J. Schachter, J. Snipes, J. Sorci, P. Stek, Y. Takase, Y. Wang, R. Watterson, J. Weaver, B. Welch, S. Wolfe, *J. Nucl. Mat.* **241-243**, 149 (1997).

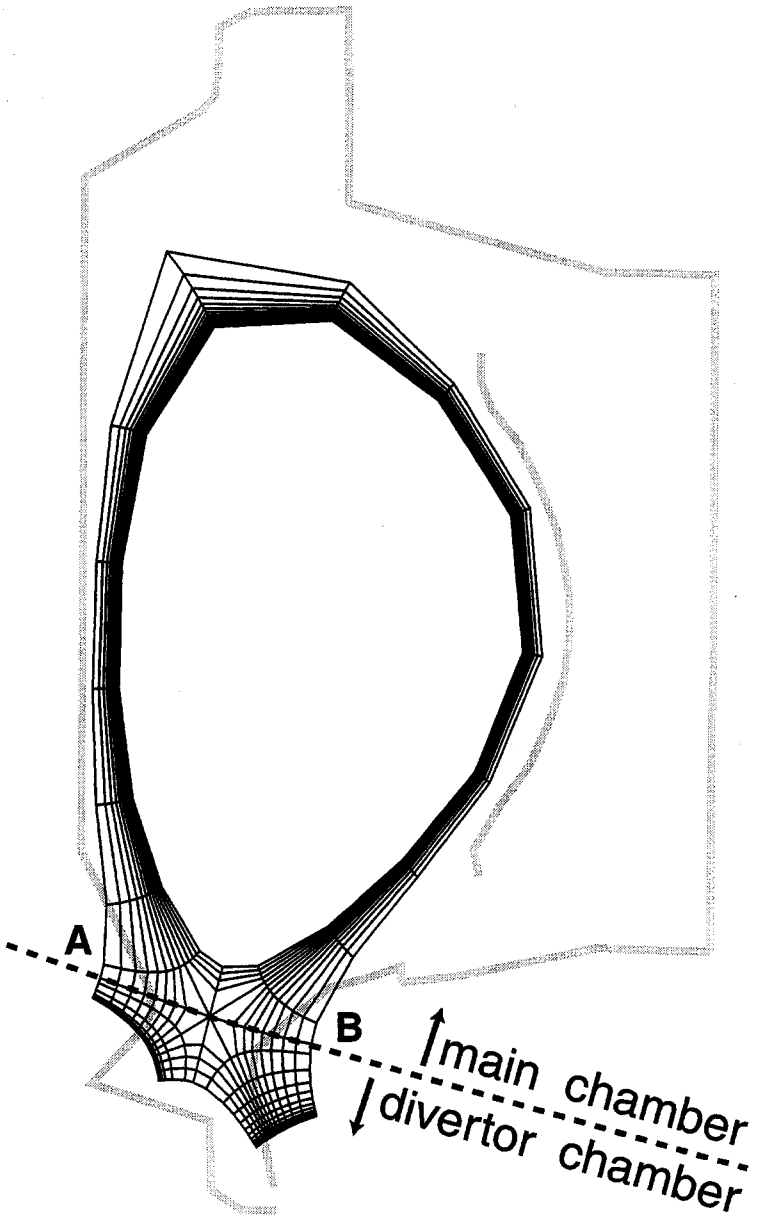

Computational mesh used in the modeling is shown with the contour of the actual wall of C-Mod in the poloidal plane. The dashed line defines the boundary between the main chamber and the divertor chamber. Divertor current Γ_d is integrated between points A and B.

Fig. 1

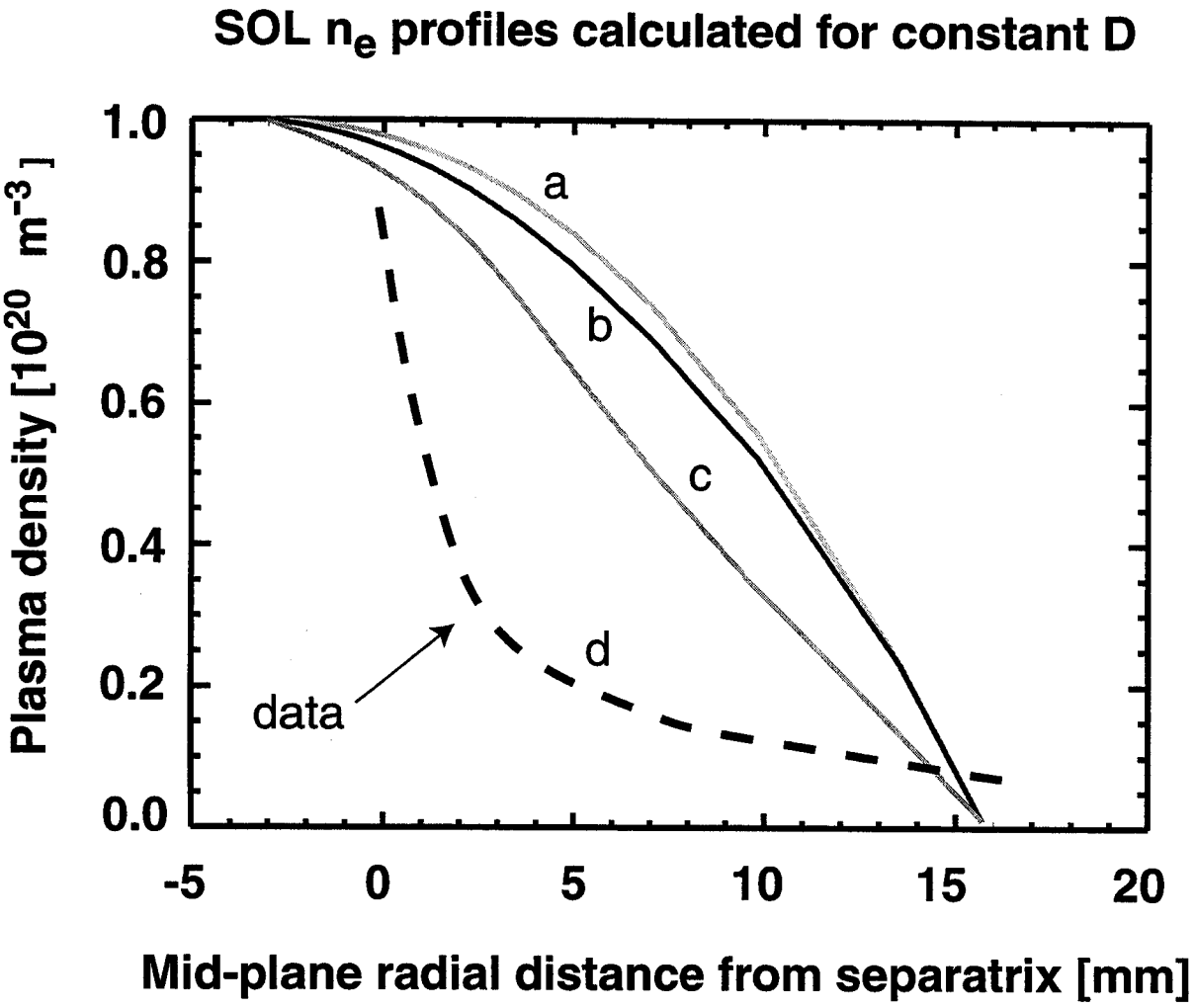

Calculated radial profiles of plasma density for spatially constant anomalous diffusion coefficient: (a) D=0.5 m^2/s, (b) D=0.1 m^2/s, (c) D=0.02 m^2/s. For all presented cases the anomalous heat diffusivity was set 0.25 m^2/s. A typical experimental profile is shown by dashed line (d).

Fig. 2

Calculated SOL profiles for high P_{mid} case

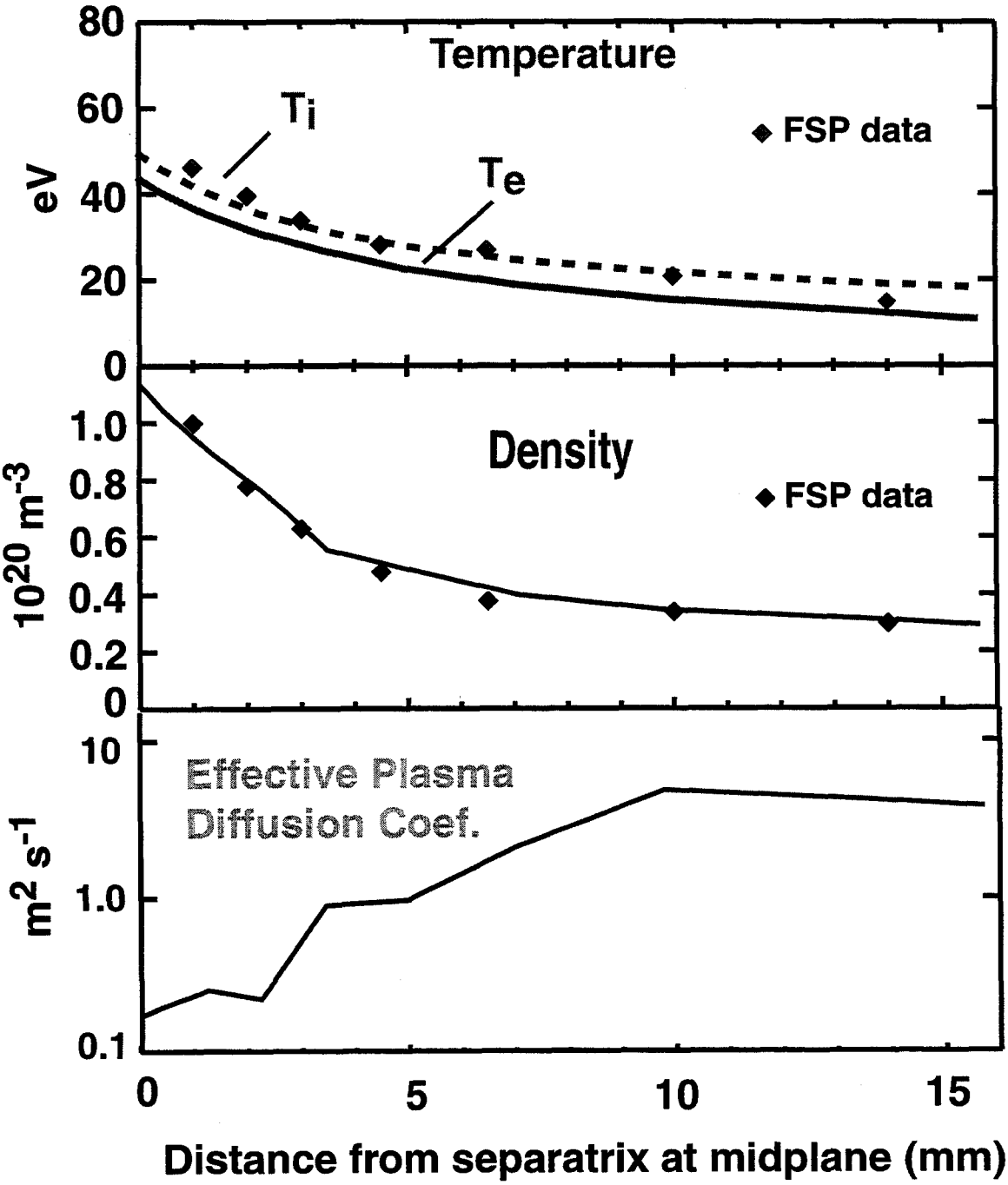

Radial profiles of n_e and T_e at the outer mid-plane are fitted to the data by using non-uniform effective plasma diffusion coefficient. Anomalous heat diffusivity is uniform (0.1 m^2/s).

Fig. 3

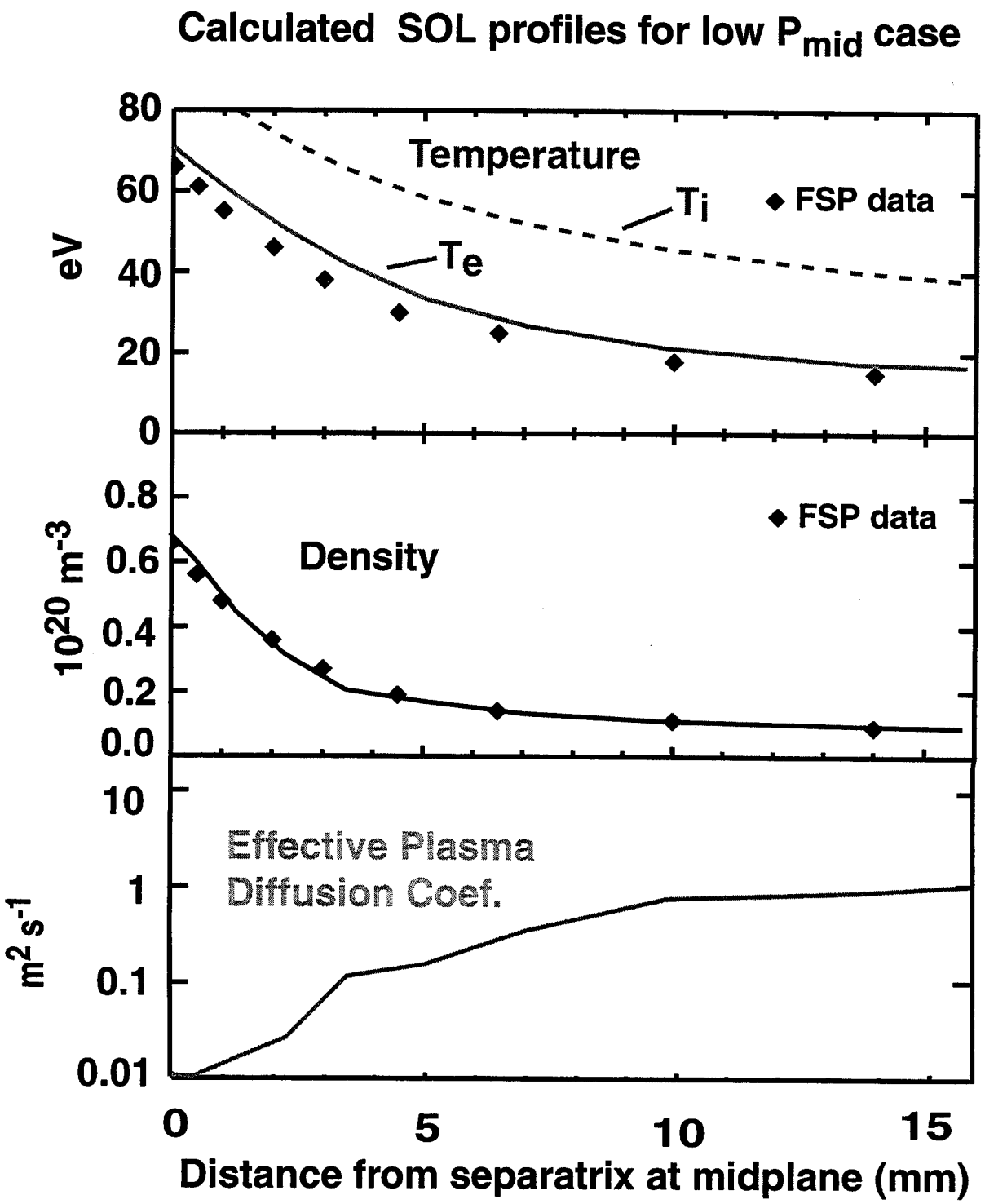

Radial profiles of n_e and T_e at the outer mid-plane are fitted to the data by using non-uniform effective plasma diffusion coefficient. Anomalous heat diffusivity is uniform (0.5 m^2/s).

Fig. 4

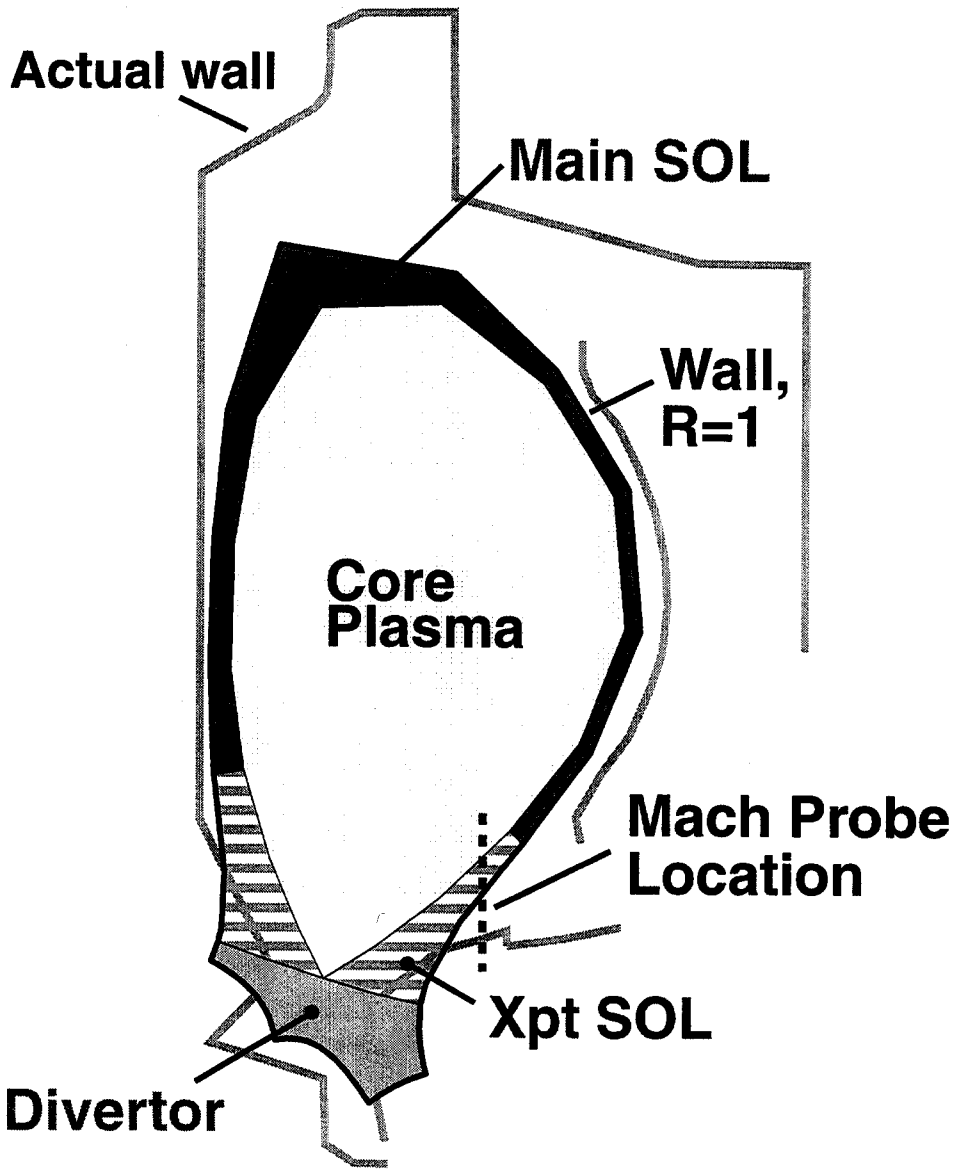

The main SOL domain is defined as the part of the SOL lying above the Mach probe location. The main SOL domain has three types of boundaries: outer wall, separatrix and the bottom which is defined as the lower edge of the main SOL domain.

Fig. 5

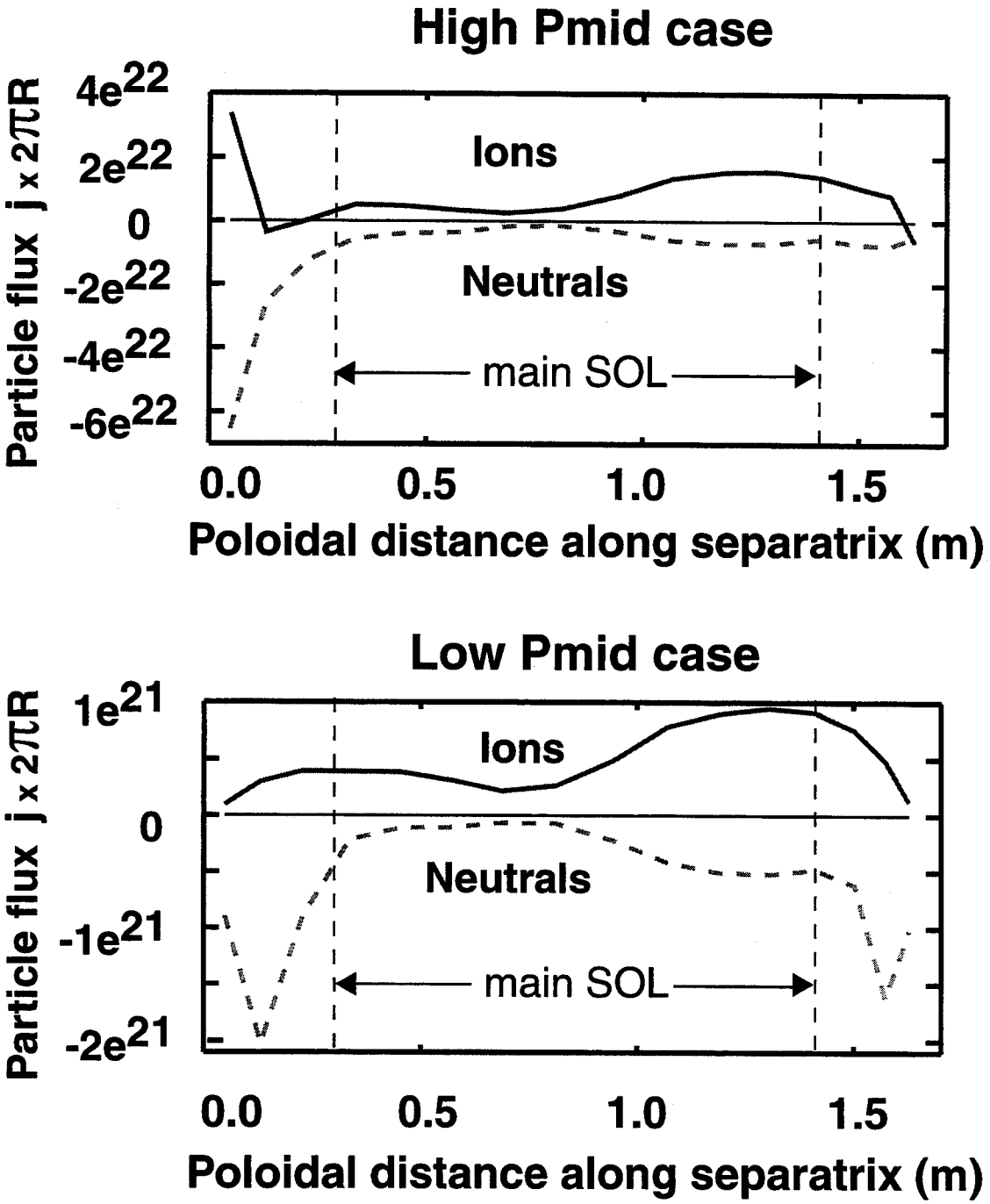

Radial particle flux density across LCFS, j, scaled by $2\pi R$, where R is the local major radius, is plotted against the length of the poloidal projection of the separatrix clockwise from x-point to x-point. The end points on the x-axis correspond to the X-point. The vertical dashed lines correspond to the boundaries of the main SOL domain. Outward flux has positive sign.

Figure 6

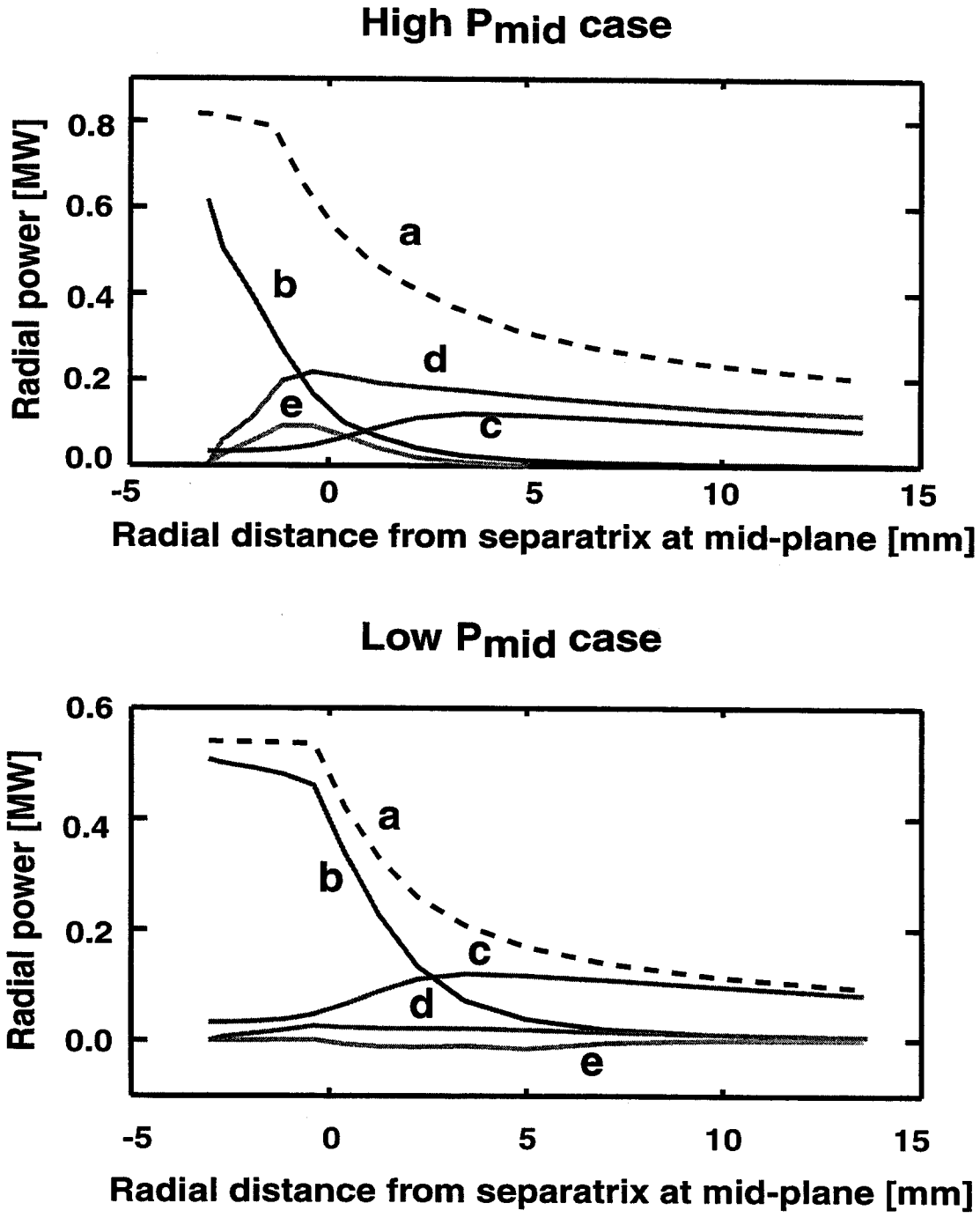

Radial heat flux in SOL: total (a), anomalous conduction (b), conduction by CX neutrals (c), convection by electons (d), convection by ions and neutrals (e).

Fig. 7

Experimental scaling of mid-plane gas pressure with core plasma density in C-Mod

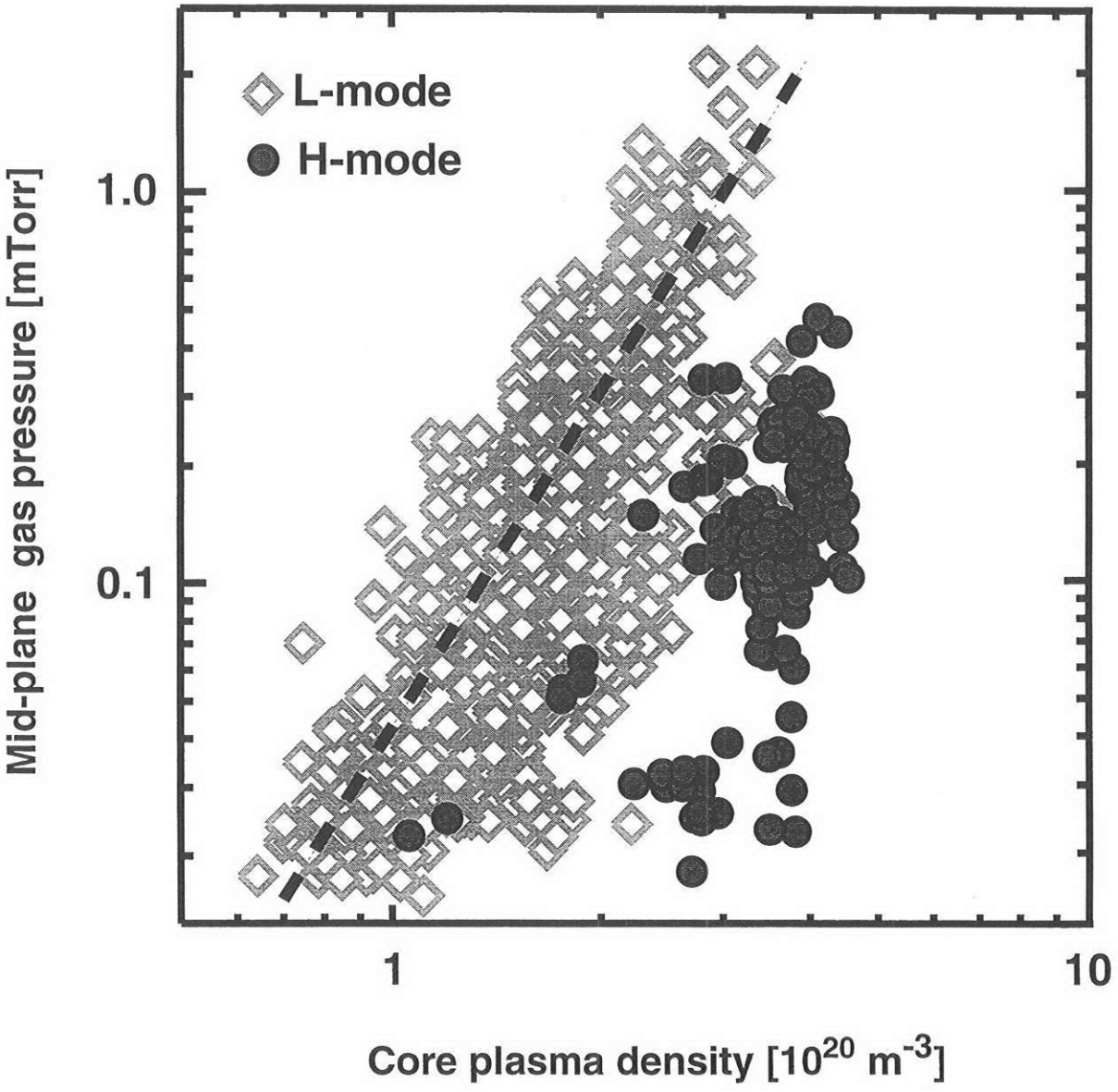

Data from about 500 shots are shown. In L-modes the mid-plane gas pressure grows approximately as the core density to the third power which implies that the anomalous transport of plasma from the core grows rapidly with the core density. The dashed line shows the best linear fit to the L-mode data.

Fig. 8